

Optimisation of confinement in a fusion reactor using a nonlinear turbulence model

E. G. Highcock,^{1,2,3} N. R. Mandell,⁴ M. Barnes,² W. Dorland,^{5,2} and JET contributors⁶

¹*Department of Physics, Chalmers University of Technology, Gothenburg, Sweden*

²*Rudolph Peierls Centre for Theoretical Physics, 1 Keble Road, Oxford, UK*

³*Culham Centre for Fusion Energy, Culham Science Centre, Abingdon, UK*

⁴*Department of Astrophysical Sciences, Princeton University, Princeton, New Jersey, USA*

⁵*Department of Physics, University of Maryland, College Park, Maryland, USA*

⁶*See the author list of Overview of the JET results in support to ITER by X. Litaudon et al. to be published in Nuclear Fusion Special issue: overview and summary reports from the 26th Fusion Energy Conference (Kyoto, Japan, 17-22 October 2016)*

(Dated: April 12, 2017)

The confinement of heat in the core of a magnetic fusion reactor is optimised using a multidimensional optimisation algorithm. For the first time in such a study, the loss of heat due to turbulence is modelled at every stage using first-principles nonlinear simulations which accurately capture the turbulent cascade and large-scale zonal flows. The simulations utilise a novel approach, with gyrofluid treatment of the small-scale drift waves and gyrokinetic treatment of the large-scale zonal flows. A simple near-circular equilibrium with standard parameters is chosen as the initial condition. The figure of merit, fusion power per unit volume, is calculated, and then two control parameters, the elongation and triangularity of the outer flux surface, are varied, with the algorithm seeking to optimise the chosen figure of merit. A two-fold increase in the plasma power per unit volume is achieved by moving to higher elongation and strongly negative triangularity.

I. INTRODUCTION

Convective heat loss resulting from micro-turbulent fluctuations in a fusion reactor limits the ability of such a reactor to confine heat to the degree required to achieve fusion. Above some critical temperature gradient, this heat loss rises extremely rapidly, effectively “pinning” the temperature gradient close to its critical value; this phenomenon is known as stiff transport (of which there are several reviews, e.g. Refs. [1–3]). With the temperature gradient limited, one way to improve fusion performance is to build larger devices, with current planning for the first demonstration power plant [4] envisioning a device more than 20 times larger by volume than the world’s largest operating test reactor, the Joint European Torus (JET). Such a tactic remains the surest route to achieving fusion with our current understanding. However, the approach is not without difficulties. First, the individual cost of such a large plant is very high (although the power output scales accordingly), putting the construction of

such reactors, as well as necessary precursor experiments and test reactors, out of the reach of all but major governments. Second, the larger designs place much greater demands upon the construction materials (see e.g. the discussion in Ref. [5]).

The reactor design effort is constantly finding innovative ways to mitigate these problems. For example, one approach to achieving more compact and cost-effective designs is to use new high-temperature superconductors which have lower cost and greater tensile strength than the superconductors used today, and which can be constructed so as to allow easy disassembly for maintenance [6].

However, while such approaches have frequently used state of the art modelling for almost all of the construction of the reactor, none of these studies have incorporated the turbulent heat loss using nonlinear models which accurately capture the essential properties of the turbulence. Instead, the vast majority use scaling laws, either inspired by dimensional arguments or extrapolated from current experiments

[6–9] (see also discussion in [10]). It is also possible to use more sophisticated “quasilinear” models [11, 12] which calculate the linear properties of the instabilities which drive the turbulence and use phenomenological rules, and calibration to a pre-determined subset of nonlinear simulations, to calculate the turbulent heat loss from these linear properties. Use of these quasilinear models includes both full reactor design studies (e.g. Refs. [13–15]) and efforts to predict and optimise performance for particular devices (e.g. Refs. [16–20]). Additionally, there have been advances in using neural-network approaches to allow such methods to fully replace the simple scaling laws by facilitating extremely fast simulation based on the quasilinear models [21]. Nonetheless, nonlinear turbulence calculations, while used routinely for investigation of individual experiments and verification of quasilinear models, have been conspicuously absent from reactor design.

The primary reason for the absence of nonlinear models is their cost and complexity. Effectively, it would have been impossible until recently to have completed a design study including these models on any reasonable timescale. However, the absence represents a missed opportunity: because simplified models of turbulent heat loss are used, a conscientious fusion designer must use pessimistic estimates in order to allow margin for error (see discussion in Ref. [10]). These pessimistic estimates cannot in general, therefore, take into account much of the last 20 years of understanding, derived from both experiment and theoretical inquiry, of the circumstances in which the levels of turbulence can be greatly reduced, without reducing the temperature gradient [22–27]. Even where designs are based on extrapolation from the best performing experimental configurations known to date (e.g. Ref. [15]), they can know nothing of potential further gains still to be had in the vast configuration space at their disposal (for one particular case, Ref. [8] showed that in theory, where full control could be maintained over turbulent transport, it was possible to reduce the capital cost of the reactor plant by 30%, that is, 10 billion (1995) US dollars, compared

to the most advanced designs of the day).

Every fusion experiment costs vast sums to build, and owing to the hard limits placed by all components of the reactor, can only explore a certain small region of the high- (or infinite-)dimensional design space. It is beholden upon theory and numerical study to search the design space, at several-orders-of-magnitude smaller expense, to identify the most promising regions. However, in order for this search to be meaningful, we must have confidence in the predictions. The simplified models used must either be pessimistic, or be used only in regimes where they have been benchmarked against more complete models or experiment and thus preclude the possibility of entirely new design paradigms. By contrast, careful comparison with experiment over recent years has provided a high degree of confidence that nonlinear models (specifically gyrokinetic models, which use a five-dimensional reduction of the Vlasov equation valid in the conditions of a fusion reactor; for a review see Ref. [28]), without any provision of tuning or fitting parameters, are able to accurately predict what the properties of turbulence will be like in a given situation [29–31].

II. A FIRST-PRINCIPLES MODEL

Here we present the first case where a first-principles nonlinear model of turbulence (specifically a novel hybrid gyrofluid/gyrokinetic model, described below, which produces excellent agreement with gyrokinetic models) has been used, as part of a multi-scale transport analysis, to calculate the performance of the core of a given configuration *ab initio* and then seek for a higher performing solution. In this particular study, the optimisation algorithm chosen achieved an improvement in the fusion power per unit volume of 91%. However, this first study is envisioned as a proof of concept, as the stepping stone for a much larger effort in which many more dimensions of parameter space are explored.

A magnetic fusion reactor is composed of a

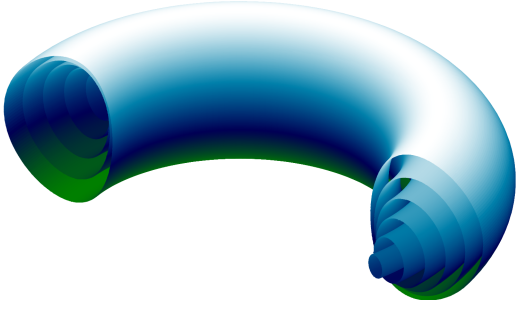


FIG. 1. An illustration of the nested magnetic flux surfaces that confine a fusion plasma.

plasma confined by a series of nested toroidal magnetic flux surfaces (Fig. 1). The plasma is composed of ionised deuterium and tritium, which fuse together to produce helium, neutrons, and a large amount of energy, provided sufficient pressure is achieved over sufficient volume in the centre of the plasma. The magnetic field is provided by a series of large external field coils and a current which flows through the plasma itself (as well as by various small coils responsible in addition for the stability of the field). The plasma is heated in a number of different ways: by the current itself, by the injection of a beam of high energy neutral particles, and by high power electromagnetic radiation of various frequencies. Fuel is injected by means of puffs of gas, frozen pellets, and neutral particle beams. Heat is lost via neutrons, radiation and by particle loss to the wall (which is concentrated in a special target region called the divertor). In this investigation we consider the core of the reactor; that is we consider the inner $\sim 90\%$ (by minor radius) of the flux surfaces. We assume the existence of an edge transport barrier, that is, that there is good confinement with a steep pressure gradient in the remaining $\sim 10\%$ of the plasma (a standard assumption since the discovery of the “high-confinement mode” [32]). We also assume that the barrier is independent of elongation and triangularity (this assumption, necessary because we are considering only core transport, differs from current experimental observations,

and is discussed further below).

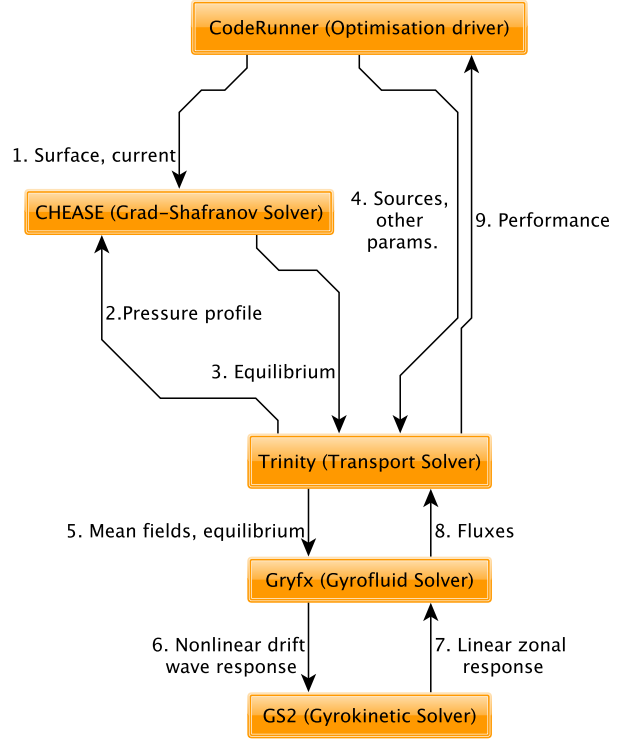


FIG. 2. Schematic of the CODERUNNER/TRINITY optimisation framework

The software used in this study to optimise such a reactor is the CODERUNNER/TRINITY optimisation framework. This is a sizeable edifice of software comprising many independent parts, as illustrated in Fig. 2. The equations underlying the framework are given in Appendix A. The calculation proceeds as follows.

The choice of optimisation control parameters, and all other requisite input information, is provided to the CODERUNNER framework, which acts as the optimisation driver. From this input, an initial configuration is assembled, comprising parameterisations of:

- the shape of the flux surface at the edge of the plasma core;
- the profile of the toroidal current, and

- the initial pressure profile, including a fixed finite pressure at the edge of the plasma core.

These are used (Link 1 in Fig. 2) by the CHEASE code [33] to calculate the shape of the magnetic flux surfaces (i.e., the equilibrium magnetic field).

For the initial configuration we consider a hypothetical tokamak with machine parameters (see Table I) and density and source profiles (both held fixed here) that are comparable in magnitude to those of the Joint European Torus (JET). Fig. 3 compares the density, source and safety factor profiles to those of JET discharge #42982, as treated in [34] and distributed in the tokamak profile database [35]. While the system of equations used in this study produces a self-consistent result without a need for these particular choices, choosing a configuration comparable in magnitude to a real experiment allows us to double-check the initial solution, by comparing the predicted temperature profile of the initial solution with that measured for discharge #42982: see Fig. 3.

The initial configuration, including the magnetic equilibrium solution, details of external heat sources and the profiles of particle density (which is held fixed) are then used (Links 2 and 3) by the TRINITY transport solver [34] to find the pressure (and thus the fusion power generated), across the whole of the plasma, with the additional assumption that the temperatures of the ions and electrons are kept equal by collisional equilibration. This is done by allowing the pressure profile to evolve until the heat losses, due to turbulence (discussed below) and other effects, match the heat inputs, both external and that generated by fusion. However, since the magnetic equilibrium itself is affected by the pressure, the result of the TRINITY calculation must be fed back to CHEASE (Link 4), a new equilibrium generated, and TRINITY re-run, until the cycle converges, the pressure stops changing and a steady-state solution is found.

To calculate the heat loss due to turbulence (Links 5 and 8), TRINITY uses several simultaneous copies of the GPU-based hybrid gyrofluid/gyrokinetic code GRYFX [37]. Each copy

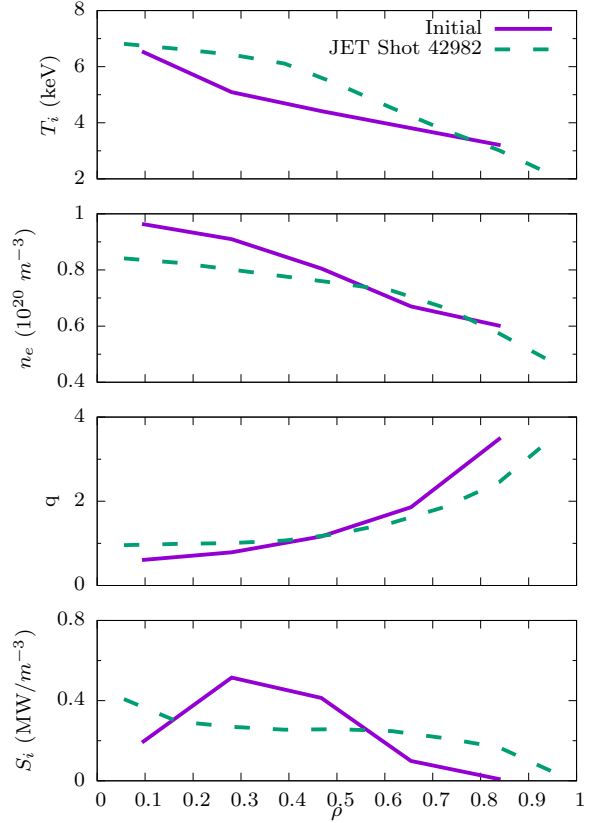


FIG. 3. This study considers a hypothetical configuration with electron density (n_e), ion heat source (S_i) and safety factor (q) profiles (here we show the initial case) comparable in magnitude to a real experiment (JET shot #42982). The calculated ion temperature (T_i) profile for the initial case agrees with the experimental case to within an order of magnitude.

of GRYFX calculates the heat flux resulting from the turbulence at a particular location in the plasma, that is, on a particular magnetic flux surface, given the pressure profile and magnetic equilibrium. A mean-field, multi-scale approach is used. The turbulent heat flux is calculated for the current pressure profile; the heat flux is then used to evolve the pressure profile, at which point the turbulent heat flux is recalculated. An illustration of the complete system is

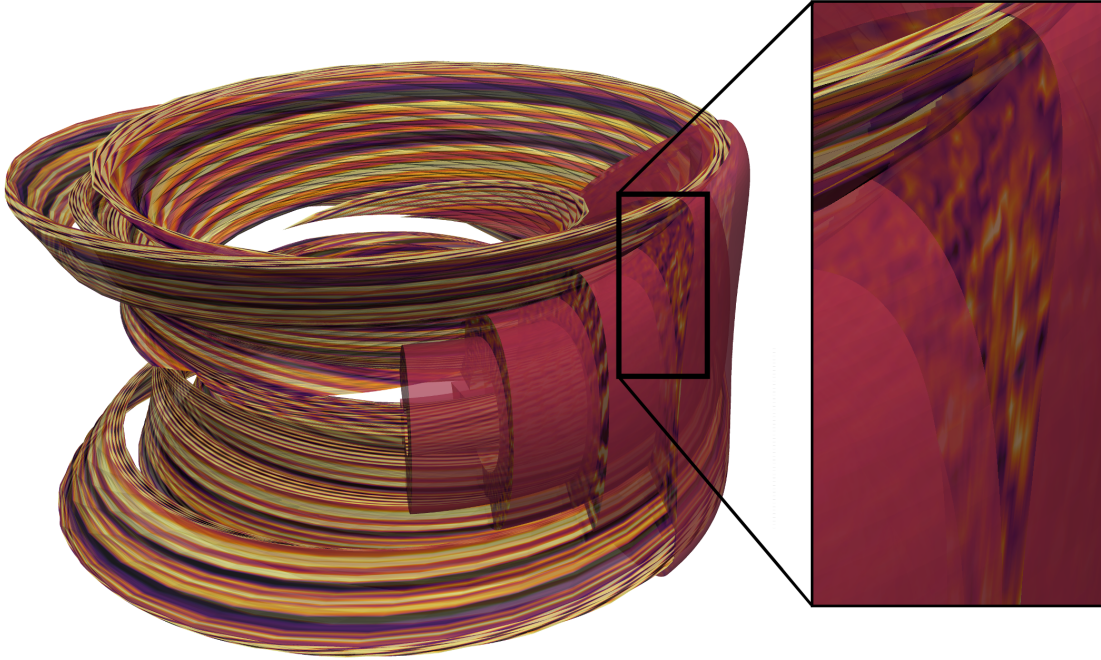


FIG. 4. An illustration of a TRINITY simulation showing above-threshold turbulence for the optimal configuration. The elongated ribbons to the left of the main picture are flux tubes [36], the domains in which the turbulence is calculated, using the local approximation which assumes the turbulent fluctuations are small-scale perpendicular to the magnetic field. Assuming statistical periodicity (which again results from the small scale of the fluctuations), these flux tubes can be repeated to fill the four flux surfaces being simulated (which are shown cut away to the right of the main picture). The picture to the right shows the cross-section of the turbulence.

given in Fig. 4.

III. FINDING THE OPTIMAL SOLUTION

The GRYFX code divides the calculation of the heat flux in two (Links 6 and 7) using a novel algorithm: the evolution of the smaller scale drift waves is calculated using the gyrofluid model [38, 39] by GRYFX, and the evolution of the large-scale zonal flows which are generated by the turbulence is calculated by the gyrokinetic code Gs2 [40, 41], with the nonlinear interaction between the two scales (and among the drift waves of various scales) being calculated in GRYFX. The simulations are electrostatic with a Boltzmann response for electrons.

When the pressure, magnetic equilibrium, and turbulent heat fluxes have ceased to evolve, a steady-state solution has been found. At this point, the figure of merit for this solution (the fusion power per unit volume) is used by the optimisation driver CODERUNNER (Link 9 in Fig. 2), to generate a new set of control parameters according to the particular optimisation algorithm being used. In this study, the Nelder-Mead simplex algorithm was selected (not to be confused with the simplex algorithm in linear programming). This is a slow but robust algorithm that constructs a simplex with $N+1$ ver-

tices in an N-dimensional configuration space and then at each stage takes the “worst” vertex and moves it to a more optimal place. Visually, one can perceive the simplex “crawling uphill” (Fig. 5).

Using the new values of the control parameters provided by the simplex algorithm (i.e. the next “guess”) the whole of the previous cycle is repeated, determining the figure of merit for this next configuration. The calculation proceeds likewise until it has converged on a maximum to within some specified tolerance (or until a prescribed number of iterations have taken place).

The two control parameters chosen were the elongation and triangularity of the outer flux surface (as defined in Ref. [33]). The shape of the magnetic field has long been known to have a marked effect on the turbulence, and the choice of these two shaping parameters in particular was motivated by pioneering experimental work on the TCV tokamak, which was designed to allow large variation in both—demonstrating a consequent large variation in performance [42].

The results are displayed at the bottom of Fig. 5. In this figure one can observe the evolution of the control parameters, starting with three initial guesses of $(\kappa, \delta) = (1.3, 0.2)$, $(1.3, 0.1)$ and $(1.4, 0.1)$. The lowest initial vertex is $(1.3, 0.2)$ with a power per unit volume (P/V) of 0.0313 MW m^{-3} . Initially the algorithm moves to higher elongation and lower triangularity, before proceeding to keep elongation roughly constant and to continue to decrease triangularity. The iteration was terminated when values of triangularity moved significantly beyond the limits of what has been seen in experiment (~ -0.65 [43]). The final, optimal value of P/V of 0.0598 MW m^{-3} with $(\kappa, \delta) = (1.6, -0.625)$. Thus, an improvement of 91% was discovered over the course of the optimisation. Since the final value of triangularity was somewhat extreme, we also provide data for an intermediate result with $(\kappa, \delta) = (1.525, -0.25)$, for which P/V is 0.0481 MW m^{-3} .

It is interesting also to consider the evolution of the confinement time, defined as the total

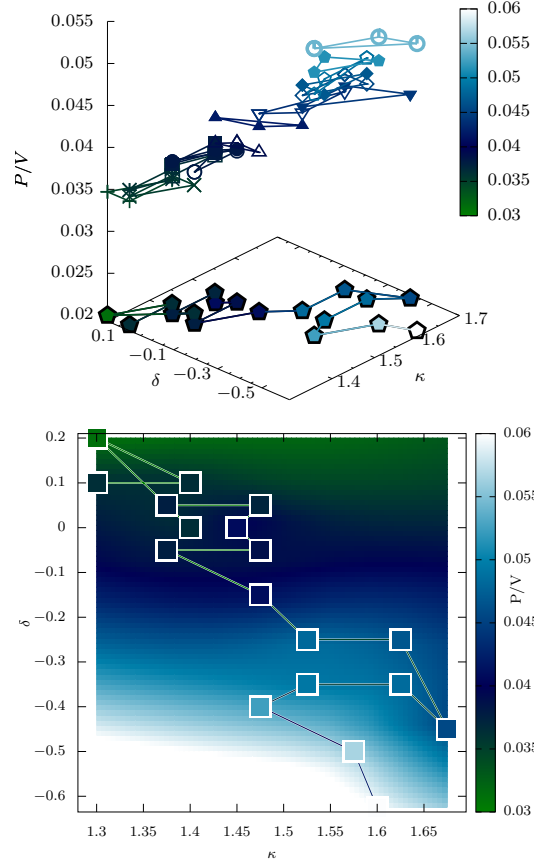


FIG. 5. *Top.* Diagram illustrating the search path taken by the simplex optimisation algorithm. The suspended triangles represent the simplex at each iteration, with the colour and height of each triangle equal to the average of the values of P/V at each of the vertices. The curve in the base plane indicates the actual sequence of function calls, that is, the actual sequence of (κ, δ) values evaluated by TRINITY. *Middle.* P/V as a function of κ and δ , both the function values (squares) and an interpolated surface, with the colour being the value of P/V . The highest (optimal) value is at $\kappa = 1.60$, $\delta = -0.625$. An intermediate solution, with a triangularity within the bounds of what has currently been realised, is chosen at $\kappa = 1.525$, $\delta = -0.25$.

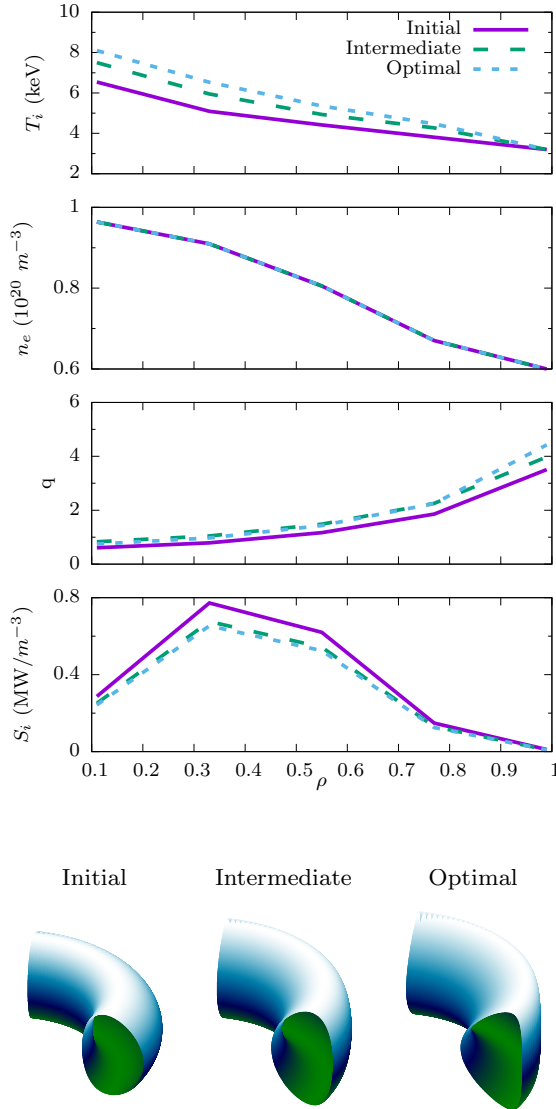


FIG. 6. *Top.* Profiles of ion temperature (T_i), electron density (n_e), safety factor (q) and heat input (S_i), showing the values of each quantity versus normalised radius ρ . ρ is a dimensionless quantity which labels the flux surface. In this work we examine core transport; thus at the outer flux surface ($\rho = 1$) there is a finite temperature of 3.2 keV and a finite electron density of $0.6 \times 10^{20} \text{ m}^{-3}$. *Bottom.* Outer flux surface shapes of the initial, intermediate and optimal solutions.

amount of stored kinetic energy divided by the rate of energy injection, is displayed in Fig. 7. We find that it is the same order of magnitude as that determined for JET #42982, given in the profile database [35] as 0.4s (the differences between the exact details of this study and the quoted case, as well as the uncertainties in determining the result, explain the discrepancy). We also see that optimising the confinement time, which reflects the ability of the system to confine heat, would have produced different results to optimising the fusion power per unit volume; in particular, the improvement at negative triangularity is less marked, and moving to higher elongation at positive triangularity may have produced a similar improvement in the confinement time.

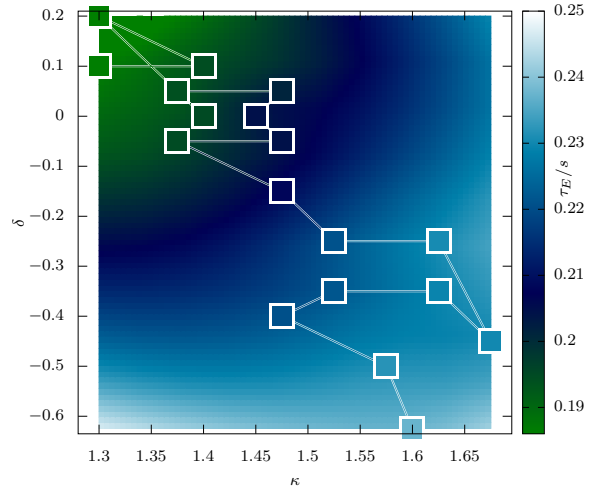


FIG. 7. Evolution of the confinement time in seconds, given as a function of elongation κ and triangularity δ . Squares represent data points, shown on top of an interpolated surface for illustration of the overall trend.

IV. DISCUSSION AND OUTLOOK

It has been shown that, without any tuning of model parameters, it has been possible to

	Initial	Intermediate	Optimal
On-axis Magnetic Field. (T)	2.91	2.84	2.81
On-axis Major Radius (m)	3.12	3.17	3.21
Ion input heat S_i (MW)	20	20	20
Plasma current I_p (MA)	1.9	1.9	1.9
Elongation κ	1.3	1.525	1.60
Triangularity δ	0.2	-0.25	-0.625
Core Volume V (m ³)	59.3	67.1	71.8
Fusion Power P (MW)	1.85	3.23	4.30
P/V (MW/m ³)	0.0313	0.0481	0.0598

TABLE I. Global properties of the initial, intermediate and optimal configurations

generate a plausible solution for reactor performance and then optimise it. The final fusion power in this study is small compared to the input heating power (on the ions) of 20MW, but that is because the parameters in this study (Tab. I) are not reactor-like, but rather of the same order of magnitude as those of JET, the largest existing device: a choice made to allow assessment of the credibility of the initial solution. Even more encouragingly, the qualitative result of this optimisation—that core confinement improved at lower triangularity and higher elongation—is directly corroborated by experimental measurements on the TCV tokamak [42] and theoretical studies [44], although as TCV is a much smaller device than that we consider here, with important effects arising from kinetic electron modes and finite gyroradius, quantitative comparisons cannot be justified.

The challenges inherent to this study, and the obstacles to such a study being carried out in the past, proceed principally from the calculation of the turbulent fluxes. All in all a total of 8680 converged nonlinear turbulence calculations at a spatial resolution of $192 \times 96 \times 20$ (radial \times poloidal \times parallel) were required. That such an exercise was possible was owing to two developments. The first was the design of the implicit algorithm in the TRINITY code which reduced the number of turbulence calculations required [34]. The second was the development of GRYFX, which by using a gyrokinetic response for the zonal flows was able to over-

come the shortcomings of gyrofluid codes in the 1990s [45] while still maintaining their huge speed advantage over gyrokinetic codes [37, 46] (discussed further in Appendix A).

It is only right to point out in this discussion that this study focuses solely on the plasma core, and not on the reactor components or the plasma edge. It should be noted that though edge transport barriers can be achieved in combination with negative triangularity [47], the evolution of the temperature at the edge of the domain, here held constant, would be strongly altered if the edge of the plasma was modelled in addition to the core, and thus the problem of optimizing the performance of the plasma as whole is distinct from optimizing that of the core, as is discussed further in [47]. Further work would be to understand how these results would be modified if the plasma edge was modelled self-consistently with the core. In light of these limitations, it would be most desirable in the future to incorporate this methodology in a holistic model of the device (including checks on magneto-hydrodynamic stability); in particular it would be desirable to control the safety factor profile to maintain values greater than one in the core to avoid the sawtooth instability (the small increase in the safety factor required is not expected to significantly affect the results presented here). However, while ultimately all parts of a tokamak must be considered, by finding ways to improve core performance, the demands placed upon the reactor design and the

requirement for high plasma confinement in the edge can be lessened.

Having demonstrated the first successful optimisation of (core) confinement using a nonlinear model of turbulence, there are several directions that are immediately attractive to follow. The first is to use this technique to find optimal configurations for JET ahead of its first run using an active (deuterium-tritium) fuel mix in twenty years (using parameters that match JET far more closely than in this study). The second is to consider, in a similar fashion, ways in which the performance of ITER, the new, global fusion experiment being constructed, can be improved. It would also be important to extend GRYFX to consider electromagnetic effects and kinetic electron physics, and to include the effects of rotation, which are not considered here. The eventual goal is to switch to using optimisation algorithms which parallelize easily and can search for global maxima, and run a vast parallel blue-skies search for a dramatically optimised fusion reactor.

V. ACKNOWLEDGEMENTS

The authors of this paper are indebted to A. Schekochihin, T. Fülöp, G. Hammett, J. Ball, J. Citrin, M. Landremann, I. Abel, F. van Wyk, F. Parra, C. Roach, S. Newton, I. Pusztai and J. Omotani for helpful discussions, ideas and support. This work has been carried out within the framework of the EUROfusion Consortium and has received funding from the Euratom research and training programme 2014-2018 under grant agreement No 633053. The views and opinions expressed herein do not necessarily reflect those of the European Commission. This work used the TACC Stampede supercomputer and the ARCHER UK National Supercomputing Service (<http://www.archer.ac.uk>).

Appendix A: Equations underlying the optimisation framework

The equations that govern the system are presented in ([28]), which builds upon an already large body of work (significantly [48, 49]).

They follow a multi-scale approach, with a clear separation in time between the evolution of the safety factor (the twist of the magnetic field lines, which evolves on the resistive timescale; [50]), the evolution of the pressure (which evolves on the confinement timescale), and the evolution of the turbulence (which occurs on the timescale of the linear micro-instabilities which drive it). The equations governing all three are

$$\frac{\partial q}{\partial t} = \frac{c}{4\pi^2} \frac{\partial}{\partial \psi} V' \langle \mathbf{E} \cdot \mathbf{B} \rangle_\psi \quad (\text{A1})$$

$$\begin{aligned} \frac{3}{2} \frac{1}{V'} \frac{\partial}{\partial t} V' \langle n_s \rangle_\psi T_s + \\ \frac{1}{V'} \frac{\partial}{\partial \psi} V' \langle Q_s \rangle_\psi = S_s \end{aligned} \quad (\text{A2})$$

and

$$\begin{aligned} \frac{\partial h_s}{\partial t} + \\ \left(v_\parallel \hat{\mathbf{b}} + \mathbf{V}_{Ds} + \frac{c}{B} \hat{\mathbf{b}} \times \nabla \langle \varphi \rangle_{\mathbf{R}} \right) \cdot \nabla h_s \\ = \langle C[h_s] \rangle_{\mathbf{R}} + \frac{Z_s e F_s}{T_s} \frac{\partial \langle \varphi \rangle_{\mathbf{R}}}{\partial t} - \\ \frac{\partial F_s}{\partial \psi} \left(\hat{\mathbf{b}} \times \nabla \langle \varphi \rangle_{\mathbf{R}} \right) \cdot \nabla \psi, \end{aligned} \quad (\text{A3})$$

respectively. In these equations, q is the magnetic safety factor, ψ is the poloidal magnetic flux which is contained within a flux surface, V is the volume of the flux surface, $V' = dV/d\psi$ is the incremental volume element (loosely, the flux surface area), \mathbf{E} is the electric field and \mathbf{B} the magnetic field, and $\langle \rangle_\psi$ denotes an average over the flux surface. The index s labels the charged particle species (e.g. electron, deuterium ion, tritium ion etc.), T_s and n_s are the species temperature and density, Q_s is the flux of heat across a flux surface, and S_s is a volumetric heat source. The quantity h_s is the

fluctuating (turbulent) part of the particle distribution function, v_{\parallel} is the velocity along the field line, $\hat{\mathbf{b}} = \mathbf{B}/|\mathbf{B}|$, \mathbf{V}_{Ds} represents the effect of the magnetic field inhomogeneities on particle motion, φ is the perturbed electric potential, C represents the effects of collisions between particles, $Z_s e$ is the species charge and F_s is the equilibrium (slowly varying) component of the species distribution function. The operator $\langle \rangle_{\mathbf{R}}$ denotes an average over gyrophase at fixed gyrocentre location \mathbf{R} . The turbulent component of the heat flux Q_s can be trivially obtained from the turbulent distribution function h_s . The (usually) sub-dominant neoclassical component of the heat flux is modelled using analytical approximations [51].

Since we are seeking a steady state solution, equation (A1) is not evolved during this study. Instead we prescribe a fixed profile of surface averaged toroidal current. This causes q to change with the pressure gradient and not on the resistive timescale during the evolution towards steady state, but once steady state is reached q ceases to evolve and the solution is self-consistent. Using the prescribed profile of toroidal current, a prescribed outer flux surface and the pressure profile, the poloidal flux (and hence the shape of the magnetic flux surfaces) can be determined using the Grad-Shafranov equation:

$$\Delta^* \psi = -4\pi R^2 \sum_s n_s T_s \left\{ \frac{d \ln n_s}{d\psi} + \frac{d \ln T_s}{d\psi} \right\} - I(\psi) \frac{dI}{d\psi}, \quad (\text{A4})$$

where Δ^* is the Grad-Shafranov operator

$$\Delta^* \psi = \left(\frac{\partial^2}{\partial R^2} - \frac{1}{R} \frac{\partial}{\partial R} + \frac{\partial^2}{\partial Z^2} \right) \psi. \quad (\text{A5})$$

Note that when using the CHEASE code ([33]) to solve the Grad-Shafranov equation, the usual function $I \partial I / d\psi$ can be replaced as an input by the surface averaged toroidal current density, which is what is specified in this study.

The equation for the pressure (A2) is evolved by TRINITY ([34]; TRINITY is also capable of evolving the density and rotation, which are kept fixed for this study). This equation determines how the evolution of the pressure is governed by the turbulent flux of heat, given sources and the shape of the magnetic flux surfaces (that is, the solution of the Grad-Shafranov equation). Since the solution of the Grad-Shafranov equation itself varies on the same timescale as the pressure, the solution is periodically updated with the new pressure profile until steady-state is reached. The pressure equation can be evolved separately for each charged species; in this study, to reduce expense, it is solved for the deuterium ions. It is then assumed that collisional processes will rapidly equilibrate the temperatures of all species, and hence that the temperatures of the electrons and tritium ions is the same as that of the deuterium ions. A fixed pressure is set at the outer magnetic flux surface ($\rho = 1$); this is set to a pressure to be expected at the edge of the core, that is, at the top of an edge transport barrier.

The turbulent distribution function, from which can be calculated the turbulent fluxes, is determined by the gyrokinetic equation (A3). This can be rigorously derived from first principles using assumptions which are valid in a fusion reactor. However, it remains too expensive to solve for the purposes of this study.

Instead, velocity space integrals are taken of this equation to create a hierarchy of fluid moments. In the early 1990s, a set of closures for this hierarchy were developed which accurately captured the linear response for drift waves, as well as finite Larmour radius effects [38, 39, 52]. Unfortunately, while successful in many cases, these “gyrofluid” models were unable to capture correctly two key properties of the turbulence, namely, the excitation of large-scale zonal flows [45] and the phenomenon of perpendicular phase mixing [53]. This resulted in the overprediction of heat fluxes by gyrofluid models. However, in recent years a new hybrid gyrofluid/gyrokinetic code has been developed, GRYFX ([37]), which overcomes these weakness,

producing excellent agreement with codes that solve the gyrokinetic equation (Fig. 8) whilst still taking orders of magnitude less time. As is described in the main text, the principle advance has been the use of a gyrokinetic solver for the linear zonal flow response, and also of new closures to capture the effects of nonlinear phase mixing. It is also important to note that recent theoretical and numerical work has showed that higher velocity space moments are energetically sub-dominant in the regimes of interest, producing renewed confidence that a closure with a sufficient number of moments can capture the important dynamics [54, 55]. In addition since GRYFX includes the full quadratic nonlinearity (the fourth term on the left hand side of equation (A3)), it is expected to capture important new phenomena such as subcritical turbulence.

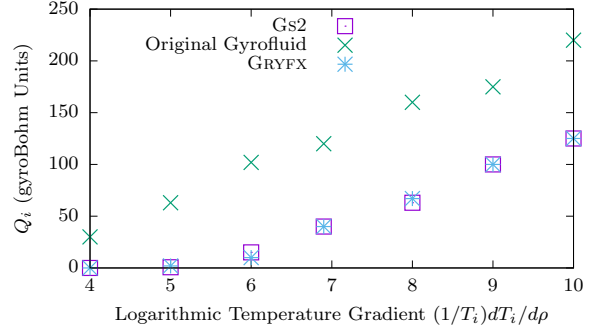


FIG. 8. Comparison between gyrokinetic simulations (Gs2), the original gyrofluid model ([39]), and GRYFX.

When using this code to calculate the turbulent fluxes within TRINITY, it is essential to use sufficient resolution to resolve the turbulent phenomena, to check for any pathologies, and to ensure that the turbulent calculation has reached convergence. There are many turbulent phenomena that can make this challenging, particularly near the threshold for the onset of turbulence, including long timescale oscillations and large amplitudes of the zonal flows.

-
- [1] G. R. Tynan, A. Fujisawa, and G. McKee, Plasma Physics and Controlled Fusion **51**, 113001 (2009).
 - [2] EJ Doyle, WA Houlberg, Y. Kamada, V Mukhovatov, TH Osborne, A Polevoi, G. Bateman, JW Connor, JG Cordey, T Fujita, X Garbet, TS Hahm, LD Horton, AE Hubbard, F Imbeaux, F Jenko, J. E. Kinsey, Y Kishimoto, J Li, TC Luce, Y Martin, M Ossipenko, V Parail, A Peeters, TL Rhodes, JE Rice, C. M. Roach, V. Rozhansky, F. Rytter, G Saibene, R Sartori, ACC Sips, JA Snipes, M Sugihara, EJ Synakowski, H Takenaga, T Takizuka, K Thomsen, MR Wade, HR Wilson, ITPA Transport Physics Topical Group, ITPA Confinement Database, Modelling Topical Group, ITPA Pedestal, Edge Topical Group, E. J. D. C. T. Physics), W. A. H. C. C. Database, Y. K. C. Pedestal, V. M. c.-C. T. Physics), T. H. O. c.-C. Pedestal, A. P. c.-C. C. Database, G. Bateman, J. W. Connor, J. G. C. (retired), T. Fujita, X. Garbet, T. S. Hahm, L. D. Horton, A. E. Hubbard, F. Imbeaux, F. Jenko, J. E. Kinsey, Y. Kishimoto, J. Li, T. C. Luce, Y. Martin, M. Ossipenko, V. Parail, A. Peeters, T. L. Rhodes, J. E. Rice, C. M. Roach, V. Rozhansky, F. Rytter, G. Saibene, R. Sartori, A. C. C. Sips, J. A. Snipes, M. Sugihara, E. J. Synakowski, H. Takenaga, T. Takizuka, K. Thomsen, M. R. Wade, H. R. Wilson, I. T. P. T. Group, I. C. Database, M. T. Group, I. Pedestal, E. T. Group, E. J. Doyle, W. A. Houlberg, Y. Kamada, V. Mukhovatov, T. H. Osborne, A. Polevoi, and J. G. Cordey, Nuclear Fusion **47**, S18 (2007).
 - [3] W. Horton, Reviews of Modern Physics **71**, 735 (1999).
 - [4] G. Federici, R. Kemp, D. Ward, C. Bachmann, T. Franke, S. Gonzalez, C. Lowry, M. Gadom-

- ska, J. Harman, B. Meszaros, C. Morlock, F. Romanelli, and R. Wenninger, *Fusion Engineering and Design* **89**, 882 (2014).
- [5] D. Stork, P. Agostini, J. L. Boutard, D. Buckthorpe, E. Diegele, S. L. Dudarev, C. English, G. Federici, M. R. Gilbert, S. Gonzalez, A. Ibarra, C. Linsmeier, A. L. Puma, G. Marbach, L. W. Packer, B. Raj, M. Rieth, M. Q. Tran, D. J. Ward, and S. J. Zinkle, *Fusion Engineering and Design* **89**, 1586 (2014).
- [6] B. N. Sorbom, J. Ball, T. R. Palmer, F. J. Mangiarotti, J. M. Sierchio, P. Bonoli, C. Kasten, D. A. Sutherland, H. S. Barnard, C. B. Haakonsen, J. Goh, C. Sung, and D. G. Whyte, *Fusion Engineering and Design* **100**, 378 (2015), arXiv:1409.3540.
- [7] N. Uckan, in *ITER Documentation Series 10 (Vienna: IAEA)* (1990).
- [8] J. Galambos, L. Perkins, S. Haney, and J. Mandrekas, *Nuclear Fusion* **35**, 551 (1995).
- [9] T. Luce, C. Challis, S. Ide, E. Joffrin, Y. Kamada, P. Politzer, J. Schweinzer, a.C.C. Sips, J. Stober, G. Giruzzi, C. Kessel, M. Murakami, Y.-S. Na, J. Park, a.R. Polevoi, R. Budny, J. Citrin, J. Garcia, N. Hayashi, J. Hobirk, B. Hudson, F. Imbeaux, a. Isayama, D. McDonald, T. Nakano, N. Oyama, V. Parail, T. Petrie, C. Petty, T. Suzuki, and M. Wade, *Nuclear Fusion* **54**, 013015 (2014).
- [10] H. Zohm, C. Angioni, E. Fable, G. Federici, G. Gantenbein, T. Hartmann, K. Lackner, E. Poli, L. Porte, O. Sauter, G. Tardini, D. Ward, and M. Wischmeier, *Nuclear Fusion* **53**, 073019 (2013).
- [11] G. M. Staebler, J. E. Kinsey, and R. E. Waltz, *Physics of Plasmas* **14** (2007), 10.1063/1.2436852.
- [12] C. Bourdelle, J. Citrin, B. Baiocchi, A. Casati, P. Cottier, X. Garbet, and F. Imbeaux, *Plasma Physics and Controlled Fusion* **58**, 014036 (2016).
- [13] G. M. Staebler and H. E. S. John, *Nuclear Fusion* **46**, L6 (2006).
- [14] R. Wenninger, F. Arbeiter, J. Aubert, L. Aho-Mantila, R. Albanese, R. Ambrosino, C. Angioni, J.-F. Artaud, M. Bernert, E. Fable, A. Fasoli, G. Federici, J. Garcia, G. Giruzzi, F. Jenko, P. Maget, M. Mattei, F. Maviglia, E. Poli, G. Ramogida, C. Reux, M. Schneider, B. Sieglin, F. Villone, M. Wischmeier, and H. Zohm, *Nuclear Fusion* **55**, 063003 (2015).
- [15] S. C. Jardin, C. E. Kessel, T. K. Mau, R. L. Miller, F. Najmabadi, V. S. Chan, M. S. Chu, R. Lahaye, L. L. Lao, T. W. Petrie, P. Politzer, H. E. St. John, P. Snyder, G. M. Staebler, A. D. Turnbull, and W. P. West, *Fusion Engineering and Design* **80**, 25 (2006).
- [16] V. Mukhovatov, Y. Shimomura, A. Polevoi, M. Shimada, M. Sugihara, G. Bateman, J. G. Cordey, O. Kardaun, G. Pereverzev, I. Voitsekhovitch, J. Weiland, O. Zolotukhin, A. Chudnovskiy, A. H. Kritz, A. Kukushkin, T. Onjun, A. Pankin, and F. W. Perkins, *Nuclear Fusion* **43**, 942 (2003).
- [17] R. V. Budny, *Nuclear Fusion* **49**, 85008 (2009).
- [18] J. E. Kinsey, G. M. Staebler, J. Candy, R. E. Waltz, and R. V. Budny, *Nuclear Fusion* **51**, 083001 (2011).
- [19] V. Parail, R. Albanese, R. Ambrosino, J. F. Artaud, K. Besseghir, M. Cavinato, G. Corrigan, J. Garcia, L. Garzotti, Y. Gribov, F. Imbeaux, F. Koechl, C. V. Labate, J. Lister, X. Litaudon, A. Loarte, P. Maget, M. Mattei, D. McDonald, E. Nardon, G. Saibene, R. Sartori, and J. Urban, *Nuclear Fusion* **53**, 113002 (2013).
- [20] O. Meneghini, P. B. Snyder, S. P. Smith, J. Candy, G. M. Staebler, E. A. Belli, L. L. Lao, J. M. Park, D. L. Green, W. Elwasif, B. A. Grierson, and C. Holland, *Physics of Plasmas* **23**, 042507 (2016).
- [21] J. Citrin, S. Breton, F. Felici, F. Imbeaux, T. Aniel, J. F. Artaud, B. Baiocchi, C. Bourdelle, Y. Camenen, and J. Garcia, *Nuclear Fusion* **55**, 92001 (2015), arXiv:1502.07402v1.
- [22] K. H. Burrell, *Physics of Plasmas* **4**, 1499 (1997).
- [23] E. J. Synakowski, *Plasma Physics and Controlled Fusion* **40**, 581 (1999).
- [24] E. G. Highcock, M. Barnes, A. A. Schekochihin, F. I. Parra, C. M. Roach, and S. C. Cowley, *Physical Review Letters* **105**, 215003 (2010).
- [25] M. Barnes, F. I. Parra, E. G. Highcock, A. Schekochihin, S. C. Cowley, and C. M. Roach, *Physical Review Letters* **106**, 1 (2011).
- [26] E. G. Highcock, A. A. Schekochihin, S. C. Cowley, M. Barnes, F. I. Parra, C. M. Roach, and W. Dorland, *Physical Review Letters* **109**, 265001 (2012).
- [27] J. Citrin, J. Garcia, T. Görler, F. Jenko, P. Mantica, D. Told, C. Bourdelle, D. R. Hatch, G. M. D. Hogeweij, T. Johnson, M. J. Pueschel, and M. Schneider, *Plasma Physics and Controlled Fusion* **57**, 014032 (2015).
- [28] I. G. Abel, G. G. Plunk, E. Wang, M. Barnes, S. C. Cowley, W. Dorland, and A. A.

- Schekochihin, Reports on progress in physics. Physical Society (Great Britain) **76**, 116201 (2013).
- [29] A. E. White, N. T. Howard, M. Greenwald, M. L. Reinke, C. Sung, S. Baek, M. Barnes, J. Candy, A. Dominguez, D. Ernst, C. Gao, a. E. Hubbard, J. W. Hughes, Y. Lin, D. Mikkelsen, F. I. Parra, M. Porkolab, J. E. Rice, J. Walk, S. J. Wukitch, and A. C.-M. Team, Physics of Plasmas **20**, 056106 (2013).
 - [30] J. Citrin, F. Jenko, P. Mantica, D. Told, C. Bourdelle, R. Dumont, J. Garcia, J. Haverkort, G. Hogewij, T. Johnson, and M. Pueschel, Nuclear Fusion **54**, 023008 (2014).
 - [31] F. van Wyk, E. G. Highcock, A. A. Schekochihin, C. M. Roach, A. R. Field, and W. Dorland, Journal of Plasma Physics **82** (2016), 10.1017/S0022377816001148, arXiv:1607.08173.
 - [32] F. Wagner, G. Fussmann, T. Grave, M. Keilhacker, M. Kornherr, K. Lackner, K. McCormick, E. R. Müller, A. Stäbler, G. Becker, K. Bernhardt, U. Ditte, A. Eberhagen, O. Gehre, J. Gernhardt, G. v. Gierke, E. Glock, O. Gruber, G. Haas, M. Hesse, G. Janeschitz, F. Karger, S. Kissel, O. Klüber, G. Lisitano, H. M. Mayer, D. Meisel, V. Mertens, H. Murmann, W. Poschenrieder, H. Rapp, H. Röhr, F. Rytter, F. Schneider, G. Siller, P. Smeulders, F. Söldner, E. Speth, K. H. Steuer, Z. Szyman-ski, and O. Vollmer, Physical Review Letters **53**, 1453 (1984).
 - [33] H. Lütjens, A. Bondeson, and O. Sauter, Computer physics communications **97**, 219 (1996).
 - [34] M. Barnes, I. G. Abel, W. Dorland, T. Gortler, G. W. Hammett, and F. Jenko, Physics of Plasmas **17**, 056109 (2010), arXiv:0901.2868.
 - [35] C. Roach, M. Walters, R. Budny, F. Im-beaux, T. Fredian, M. Greenwald, J. Stillerman, D. Alexander, J. Carlsson, J. Cary, F. Rytter, J. Stober, P. Gohil, C. Greenfield, M. Murakami, G. Bracco, B. Esposito, M. Romanelli, V. Parail, P. Stubberfield, I. Voitsekhovitch, C. Brickley, A. Field, Y. Sakamoto, T. Fujita, T. Fukuda, N. Hayashi, G. Hogewij, A. Chudnovskiy, N. Kinerva, C. Kessel, T. Aniel, G. Hoang, J. Ongena, E. Doyle, W. Houlberg, and A. Polevoi, Nuclear Fusion **48**, 125001 (2008).
 - [36] M. A. Beer, S. C. Cowley, and G. W. Hammett, Physics of Plasmas **2**, 2687 (1995).
 - [37] N. Mandell and W. Dorland, in *Bulletin of the American Physical Society* (2014) p. Abstract CP8.039.
 - [38] W. Dorland and G. W. Hammett, Physics of Fluids B-Plasma Physics **5**, 812 (1993).
 - [39] M. A. Beer and G. W. Hammett, Physics of Plasmas **3**, 4046 (1996).
 - [40] W. Dorland, F. Jenko, M. Kotschenreuther, and B. N. Rogers, Physical review letters **85**, 5579 (2000).
 - [41] M. Kotschenreuther, G. Rewoldt, and W. M. Tang, Computer Physics Communications **88**, 128 (1995).
 - [42] H. Weisen, S. Alberti, S. Berry, R. Behn, P. Blanchard, P. Bosshard, F. Bühlmann, R. Chavan, S. Coda, C. Deschenaux, M. J. Dutch, B. P. Duval, D. Fasel, A. Favre, S. Franke, I. Furno, T. Goodman, M. Henderson, F. Hofmann, J.-P. Hogge, P.-F. Isoz, B. Joye, J. B. Lister, X. Llobet, J.-C. Magnin, P. Mandrin, B. Marletaz, P. Marmillod, Y. Martin, J.-M. Mayor, J.-M. Moret, C. Nieswand, P. Paris, A. Perez, Z. a. Pietrzyk, V. Piffel, R. a. Pitts, A. Pochelon, K. Razumova, H. Reimerdes, A. Refke, J. Rommers, I. Roy, O. Sauter, W. Suttrop, W. V. Toledo, G. Tonetti, M. Q. Tran, F. Troyon, P. Vyas, and D. J. Ward, Plasma Physics and Controlled Fusion **39**, B135 (1999).
 - [43] A. Pochelon, T. Goodman, M. Henderson, C. Angioni, R. Behn, S. Coda, F. Hofmann, J.-P. Hogge, N. Kirneva, A. Martynov, J.-M. Moret, Z. A. Pietrzyk, F. Porcelli, H. Reimerdes, J. Rommers, E. Rossi, O. Sauter, M. Q. Tran, H. Weisen, S. Alberti, S. Barry, P. Blanchard, P. Bosshard, R. Chavan, B. P. Duval, Y. V. Esipchuck, D. Fasel, A. Favre, S. Franke, I. Furno, P. Gorg-erat, P.-F. Isoz, B. Joye, J. Lister, X. Llobet, J.-C. Magnin, P. Mandrin, A. Manini, B. Marlétaz, P. Marmillod, Y. Martin, J.-M. Mayor, J. Mlynar, C. Nieswand, P. Paris, A. Perez, R. Pitts, K. Razumova, A. Refke, E. Scavino, A. Sushkov, G. Tonetti, F. Troyon, W. V. Toledo, and P. Vyas, Nuclear Fusion **39**, 1807 (1999).
 - [44] A. Marinoni, S. Brunner, Y. Camenen, S. Coda, J. P. Graves, X. Lapillonne, A. Pochelon, O. Sauter, and L. Villard, Plasma Physics and Controlled Fusion **51**, 055016 (2009).
 - [45] A. M. Dimits, G. Bateman, M. A. Beer, B. I. Cohen, W. Dorland, G. W. Hammett, C. Kim, J. E. Kinsey, M. Kotschenreuther, a. H. Kritz, L. L. Lao, J. Mandrekas, W. M. Nevins, S. E.

- Parker, a. J. Redd, D. E. Shumaker, R. Sydora, and J. Weiland, *Physics of Plasmas* **7**, 969 (2000).
- [46] N. Mandell, W. Dorland, E. Highcock, and G. Hammett, in *Bulletin of the American Physical Society* (2016) p. Abstract TP10.23.
- [47] A. Pochelon, P. Angelino, R. Behn, S. Brunner, S. Coda, N. Kirneva, S. Medvedev, H. Reimerdes, J. Rossel, O. Sauter, L. Villard, D. Wagner, A. Bottino, Y. Camenen, G. P. Canal, P. K. Chattopadhyay, B. P. Duval, A. Fasoli, T. P. Goodman, S. Jolliet, A. Karpushov, B. Labit, A. Marinoni, J. M. Moret, A. Pitzschke, L. Porte, M. Rancic, and V. S. Udintsev, *Plasma and Fusion Research* **7**, 1 (2012).
- [48] E. A. Frieman and L. Chen, *Physics of Fluids* **25**, 502 (1982).
- [49] H. Sugama and W. Horton, *Physics of Plasmas* **5**, 2560 (1998).
- [50] I. G. Abel and S. C. Cowley, *New Journal of Physics* **15** (2013), 10.1088/1367-2630/15/2/023041, arXiv:1210.1417.
- [51] C. S. Chang and F. L. Hinton, *Physics of Fluids* **25**, 3314 (1982).
- [52] G. W. Hammett and F. W. Perkins, *Physical review letters* **64**, 3019 (1990).
- [53] T. Tatsuno, W. Dorland, A. A. Schekochihin, G. G. Plunk, M. Barnes, S. C. Cowley, and G. G. Howes, *Physical Review Letters* **103**, 2 (2009), arXiv:0811.2538.
- [54] A. A. Schekochihin, J. T. Parker, E. G. Highcock, P. J. Dellar, W. Dorland, and G. W. Hammett, *Journal of Plasma Physics* **82**, 905820212 (2016), arXiv:1508.05988.
- [55] J. T. Parker, E. G. Highcock, A. A. Schekochihin, and P. J. Dellar, *Physics of Plasmas* **23**, 070703 (2016), arXiv:1603.06968.